Effect of Eccentric Field-shaper on Electromagnetic Crimping of Terminal Wire Interconnections

Ashish K. Rajak[1*], Ramesh Kumar[1], Sachin D. Kore[1]

[1]Department of Mechanical Engineering, Indian Institute of Technology, Guwahati, Assam, India
*Corresponding author. Email: a.rajak@iitg.ernet.in

Abstract

With the increase in losses in electric power transmission in crimped terminal-wire interconnections, due to improper crimping using conventional crimping process, it is essential to find a more efficient crimping technique. Some crucial challenges in conventional terminal-wire crimping process are spring back of terminal on tool relaxation, non-uniform terminal deformation due to tool-terminal contact process, flash out of material, voids between the wire strands etc. To overcome these problems Electromagnetic crimping process is found to be a most suitable technique. In this work, an eccentric geometry field-shaper is used for electromagnetic crimping of aluminium terminal over the aluminium wires which hasn't been used yet in this field. Numerical simulations were carried out using LSDYNA^{TM} Electromagnetic module software. Results like current density, magnetic field, Lorentz force, and terminal deformation were discussed. The results from the numerical simulations were used for carrying out experiments. The validation was carried out using terminal deformation and terminal-wire contact length. The result of the work will be useful for electromagnetic crimping, welding and cladding process for similar applications.

Keywords

Electromagnetic terminal-wire crimping, Field-shaper, Finite element method Introduction

1   Introduction

Electromagnetic crimping (EMC) is one of the high-speed forming methods, used to improve the material formability beyond their conventional forming limits and to be excellent in solving the problem of forming lightweight metals that are difficult to shape at room temperature (Psyk et al., 2011). Electromagnetic terminal-wire crimping (EMTWC) is one of the electromagnetic joining processes in which the cable is stripped, and the wire strands are placed inside a metal terminal, where the metal terminal is compressed over the wire strands ensuring good electrical connectivity and mechanical strength across the joints (Rajak and Kore, 2017). Conventional crimper achieves the terminal-wire crimping process, but the disadvantage is that the crimper deteriorates the material and if the pressure gets relaxed or partially released during the process results in weak contact between the wires, thus increasing the resistivity and considerable losses in the wiring system. Moreover, compressed defects also shorten the lifespan of the terminal caused due to high temperature and electrical corrosion (Zhmurkin, 2009). The EMTWC process can be an alternative choice due to the advantage of the non-contact process, low mould cost, no lubrication, higher deformation for low formability material and less spring back phenomena (Padmanabhan, 1997).

Field-shaper is a vital tool in EM crimping process to enhance the magnetic field into the desired region for an efficient and higher deformation of the workpiece placed in the vicinity of the effective working length (Zhang et al., 1995). In this article, the effect of the eccentric field-shaper on terminal-wire crimping process is studied. As no such design of field-shaper is addressed until now in EMC process, so work is carried out using numerical and experimental approach. The simulation on EMTWC process is carried out on LS-DYNA[TM] EM module software. The general objective is to study the parameters like a magnetic field, Lorentz force, current density and deformation at various discharge voltages. Validation of the simulation is carried out using terminal radial deformation.

2   Working Principle and Modelling

An EMTWC process system consists of an electrical pulsed power circuit responsible for the generation of the pulse current flowing through the work coil. Although field-shapers seem to be a mechanical part, it plays an important role modifying the magnetic field distribution generated on the workpiece as stated by Suzuki et al. (Suzuki et al., 1987). In this process, the electrical energy stored in the capacitor bank discharges into the coil when the trigger switch closes, which allows the pulsed current to flow through the coil as shown in **Figure 1**. The current in the primary coil will induce a secondary current in the field-shaper. This secondary current will flow through the field shapers outer surface to the inner surface, thus inducing another secondary current in the adjacent terminal. As, a result of the interaction of the induced currents in the surface of the workpiece with the applied

field, a magnetic pressure is exerted on the workpiece, and it consequently helps in efficient crimping operations.
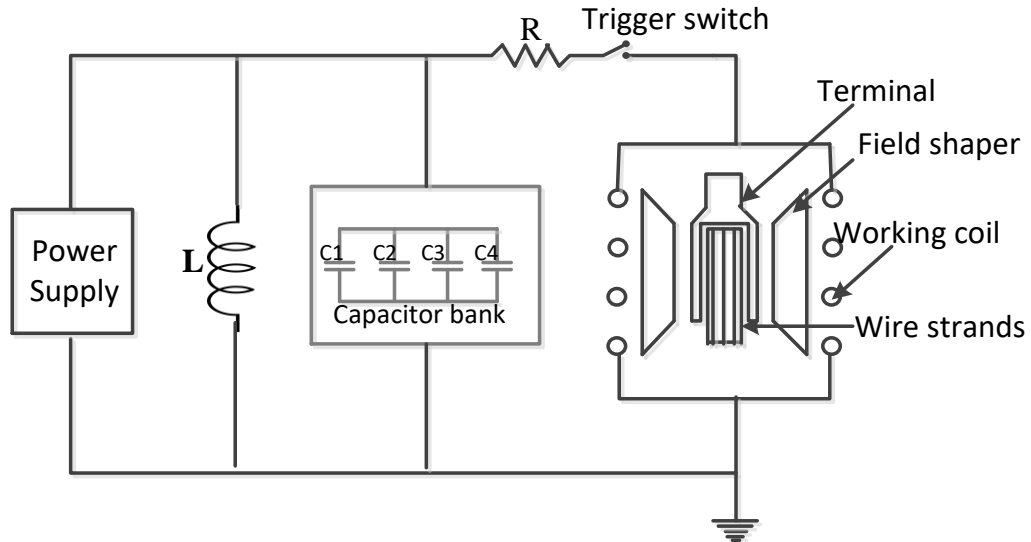

Figure 1: *Schematic diagram of a working electromagnetic terminal- wire crimping process*

In fact a field-shaper is a practical tool, which helps to concentrate the magnetic flux and efficiently prolong the service life of the coil. As reported in research paper (Bahmani et al., 2009) mathematical formulation even after inserting field-shaper between the coil and workpiece does not change. Field-shaper acts just as another metallic body and thereby, an eddy current is induced over the surface resulting in secondary induced current over the surface of the workpiece, which causes the change in the distribution of the applied electromagnetic pressure over the workpiece.

2.1   Numerical Modelling

The coupled EM and structural, mechanical numerical analysis for the terminal-wire crimping with eccentric field-shaper were carried out in LS-DYNA^{TM} EM module. The solver computes the electromagnetic fields by solving Maxwell's equations in the conductor, calculating the eddy current and Lorentz force using finite element method coupled with the boundary element method for the surrounding air (L'Eplattenier et al., 2008). The simulation computes the EM field under each step of the time increment. A total of 8 contacting parts in the model, needs 18 contact pairs for all possible two surface combination. A seven wire strands were used in the model as shown in **Figure 2**. The deformable wire strands and the terminals were modelled with C3D8R, eight-node elements. The field-shaper part was modelled using R3D4 elements. The EM crimping process is a high strain rate process so; simplified Johnson-Cook material model was used as the material model for the simulation, where the effect of temperature is assumed negligible.
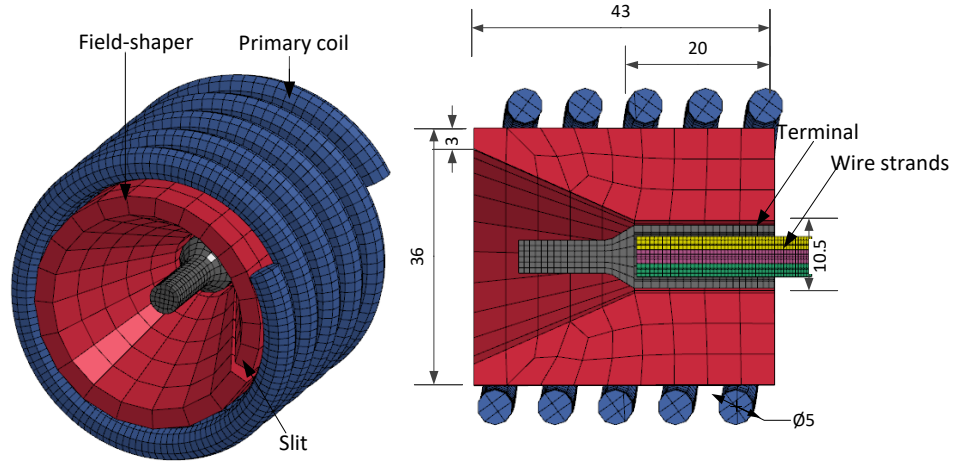
Figure 2: Modelled and cross-sectional view showing dimensions of a field shaper

The simplified Johnson-Cook constitutive relation is expressed by equation,

$$\sigma = (A + B\,\varepsilon^n)\left[1 + C\,\ln\left(\frac{\dot{\varepsilon}}{\dot{\varepsilon}_o}\right)\right]\left[1 - \left(\frac{T - T_{room}}{T_m - T_{room}}\right)^n\right] \tag{1}$$

Where σ is the equivalent plastic stress (MPa), T is the temperature (K), T_m is the melting temperature, and T_{room} is the room temperature (K) A, B, C, m and n are material constants, ε is the equivalent plastic strain, $\dot{\varepsilon}$ is the equivalent plastic strain rate (s^{-1}), ($\dot{\varepsilon}_o$) is the reference equivalent plastic strain rate (s^{-1}). Johnson-Cook model parameters are given in **Table 1**.

Table 1: Values of Johnson-Cook material constant parameter (Hustad and Lindland 2014)

Materials	A (MPa)	B (MPa)	n	C	T_m (K)	m
1050AA	110	150	0.36	0.014	918	1
Cu	90	292	0.31	0.025	1331	1.09

2.2 Materials and Procedure

The wire strands and terminal were made of AA 1050, where Johnson-Cook material property was used while working coil and field-shaper material was assigned to be copper. The mechanical and electrical properties of the materials used in the simulation are listed in **Table 2**.

*Table 2: Material properties of the coil/field-shaper and workpiece*

Parameters	Coil/ field-shaper	Workpiece
Material	Copper	AA 1050
Conductivity (S/m)	59.6×10^6	36.8×10^6
Density (Kg/m^3)	8960	2700
Poisson's ratio	0.27	0.33

The input circuit condition was based on the experimental setup, and the dimension of the workpiece is shown in **Table 3**. In EMC process, the input current was measured using a Rogowski coil which was taken from the experimental electromagnetic forming setup for various discharge voltages as shown in **Figure 3**. This input current was used as loading curve in the software to analyse the dynamic plastic deformation of the terminal.

As in EM process, the first period of the current is responsible for considerable deformation as stated by Haiping and Chunfeng (Haiping and Chunfeng, 2009). Therefore, to reduce the total FEM and BEM calculation time, the simulation was carried out for the first pulse only. The field-shaper was manufactured as per the dimensions used in the simulation as shown in **Figure 4**. Crimped samples carried out using different field-shaper are shown in **Figure 5**.

Table 3*: Circuit parameters and workpiece dimensions*

Circuit	Capacitance	90 µF
	Maximum voltage	15 kV
	Maximum energy	10 kJ
Workpiece	Material	Aluminum
	Outer diameter of terminal	9.0 mm
	Thickness of terminal	1.0 mm
	Length	20 mm
	Wire strands diameter	5.8 mm
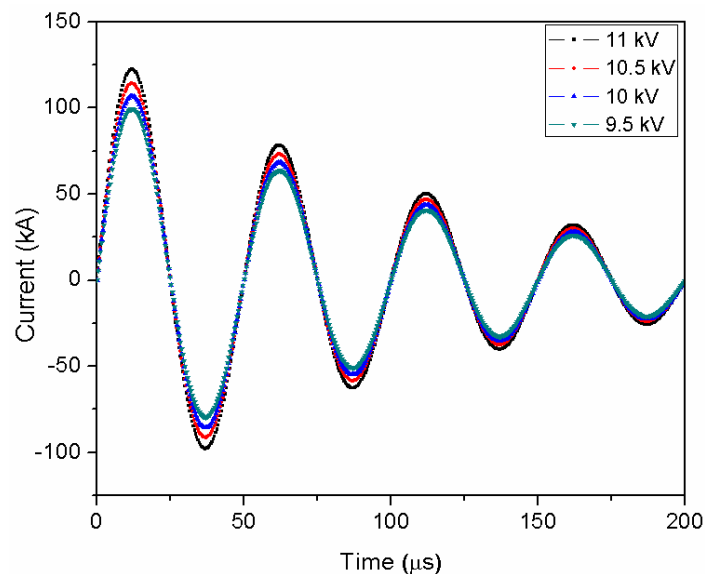
Figure 3*: Typical waveform showing current values for various discharge voltages*

LHS View   Top View   RHS View
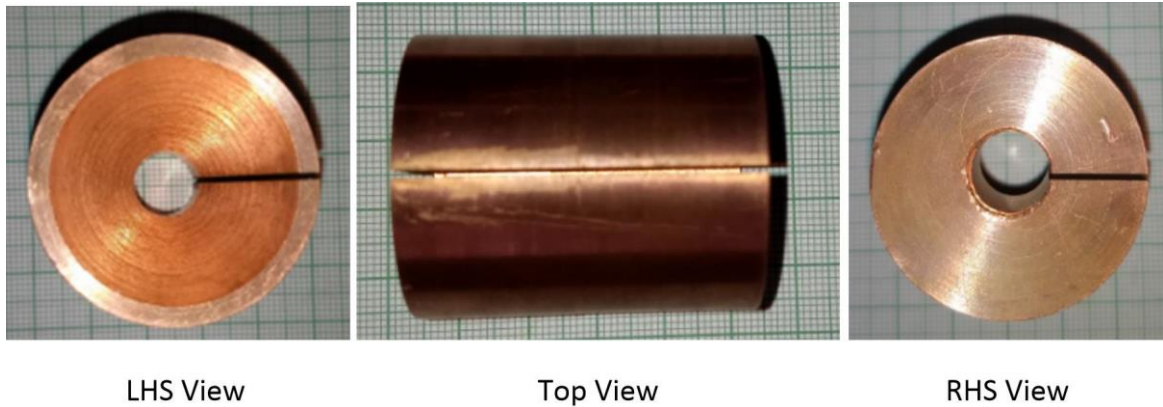
Figure 4: *Field-shapers used for carrying out experiments*

9.5 kV 10 kV 10.5 kV 11 kV

Figure 5: *Samples crimped using different types of field-shaper at various discharge voltages*

3   Results and Discussion

3.1   Current Density

In the electromagnetic system, the discharge current in the working coil can be expressed in the approximate form by equation (2),

$$I = V \sqrt{\frac{C}{L}} e^{(-\beta t)} sin(\omega t) \tag{2}$$

Where V is the initial voltage discharged from the circuit, C is the total value of the capacitor bank, L is the equivalent inductance, β is the damping coefficient, ω is the angular frequency, and t is the time period. So, as the voltage increases, the current amplitude increases and thus the induced current density on the conductor increases. It was found that, when the current is passed through the working coil around the field-shaper, the

current density induced increases. The fringe pattern of current density over the effective working zone for all the three field-shapers at 11 kV of discharge voltage is shown in **Figure 6**(a).

(a) Current density   (b) Magnetic field   (c) Lorentz force
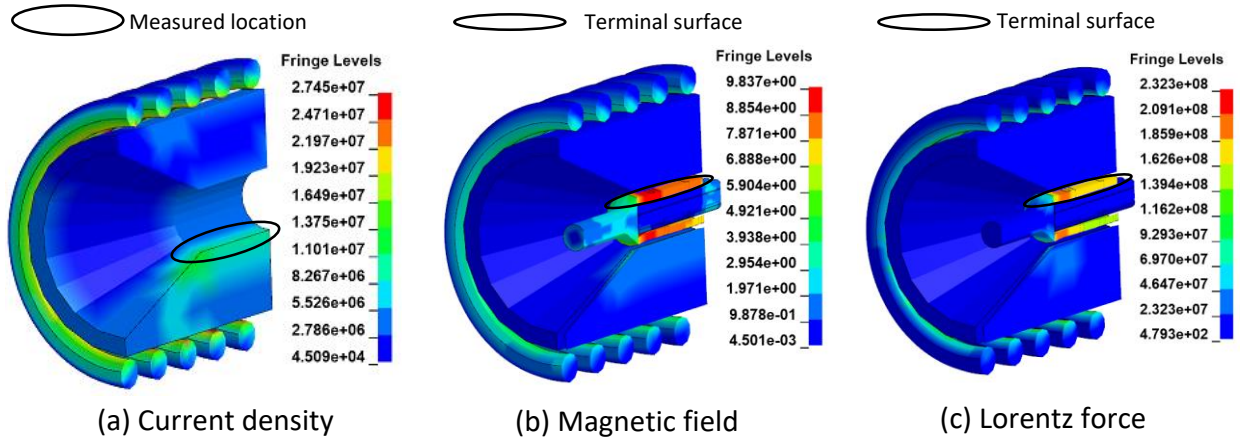
*Figure 6: Fringe pattern of (a) Current density, (b) Magnetic field, and (c) Lorentz force obtained at 11 kV*

With the increase in the discharge voltage, the peak value of the discharge current also increases, the corresponding variation in the current density with the discharge voltage is shown in **Figure 7**. The current density obtained at 11 kV in the effective working zone of the field-shaper was 27.45 kA/mm^2.
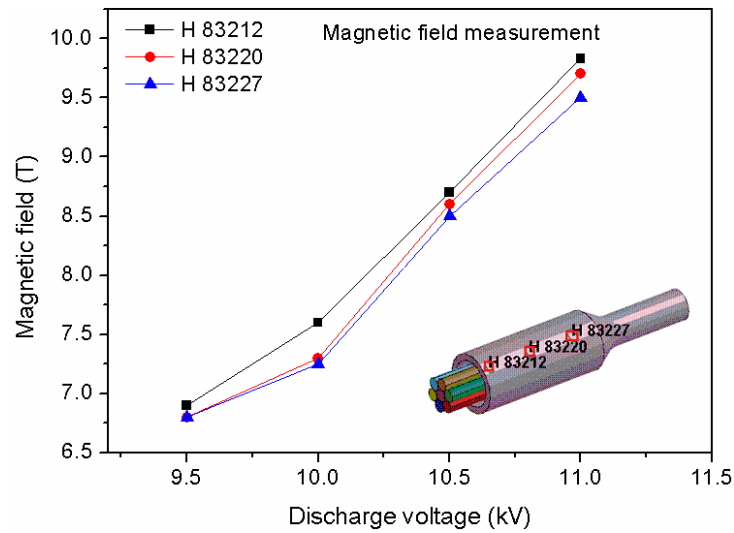
3.2 Magnetic Field

The magnetic field inside a solenoid coil is given by equation (3),

$$H_o(t) = \frac{n}{l}I(t) \qquad\qquad (3)$$

The magnetic field is dependent on the coil current as a function of time *I (t)* and the number of turns per unit length *n/l*. The magnetic field strength is directly proportional to the coil current. The higher the coil current, the higher the magnetic field. Fringe pattern of pattern of the magnetic field is shown in **Figure 6**(b). From the simulation results, it was found that magnetic field increases with the increase in current amplitude passed through the coil. In **Figure 8**, the magnetic field induced over the terminal surface for 11 kV discharge voltage was found to be 12.64 Tesla. The value of magnetic field kept on increasing with the increase in discharge voltage. According to Maxwell equations, field gradient can be expressed in terms of current density. So, the high value of current density, it increases the magnetic field.
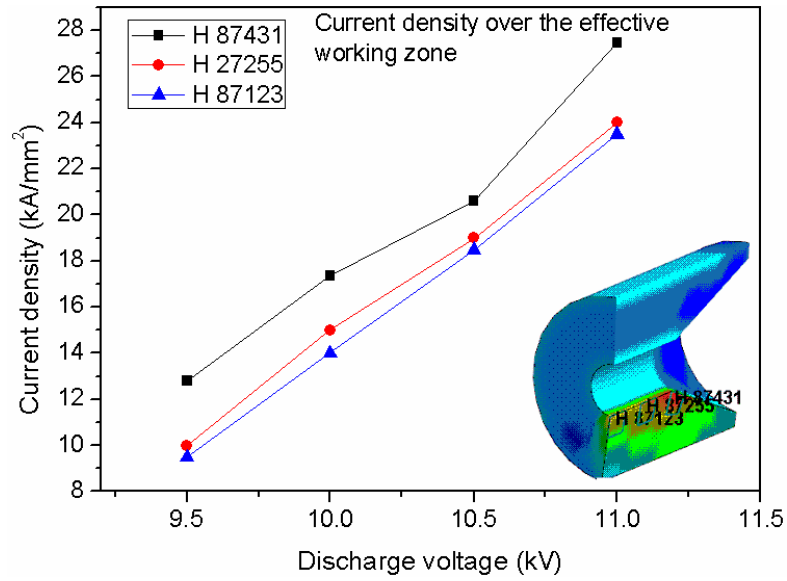
Figure 7: Variation of current density with the discharge voltage

Figure 8: Magnetic field measured over the terminal surface obtained at 11 kV
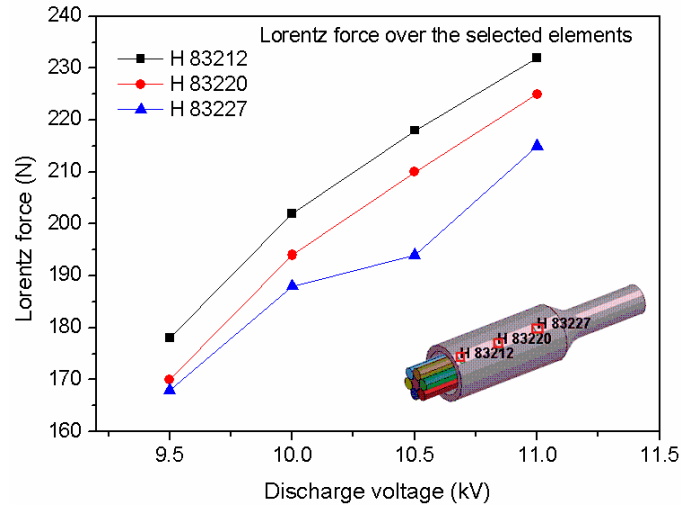
3.3 Lorentz Force

Lorentz force, *F* is the result of a combination of forces due to the electric and magnetic force, and it can be expressed by equation (6).

$$\vec{F} = q\vec{E} + q\,\vec{v} \times \vec{B} \qquad (6)$$

Where *q* is the charged particle, v is the velocity of the charged particle, *E* is the electric field and *B* is the magnetic field. The first term of the above equation is the force generated by the electric field and the second term is the force generated by the magnetic field. So it

can be seen that the Lorentz force is directly proportional to the electric field and the magnetic field. Fringe pattern of Lorenz force over the terminal is shown **Figure 6**(c).


Figure 9: *Variation of magnitude of Lorentz force for different discharge voltages*

As shown in **Figure 9**, the value of Lorentz force over the terminal surface was found to increase with the increase in discharge voltage. It was found that for 11 kV of the discharge voltage maximum Lorentz force of 232 N was obtained.
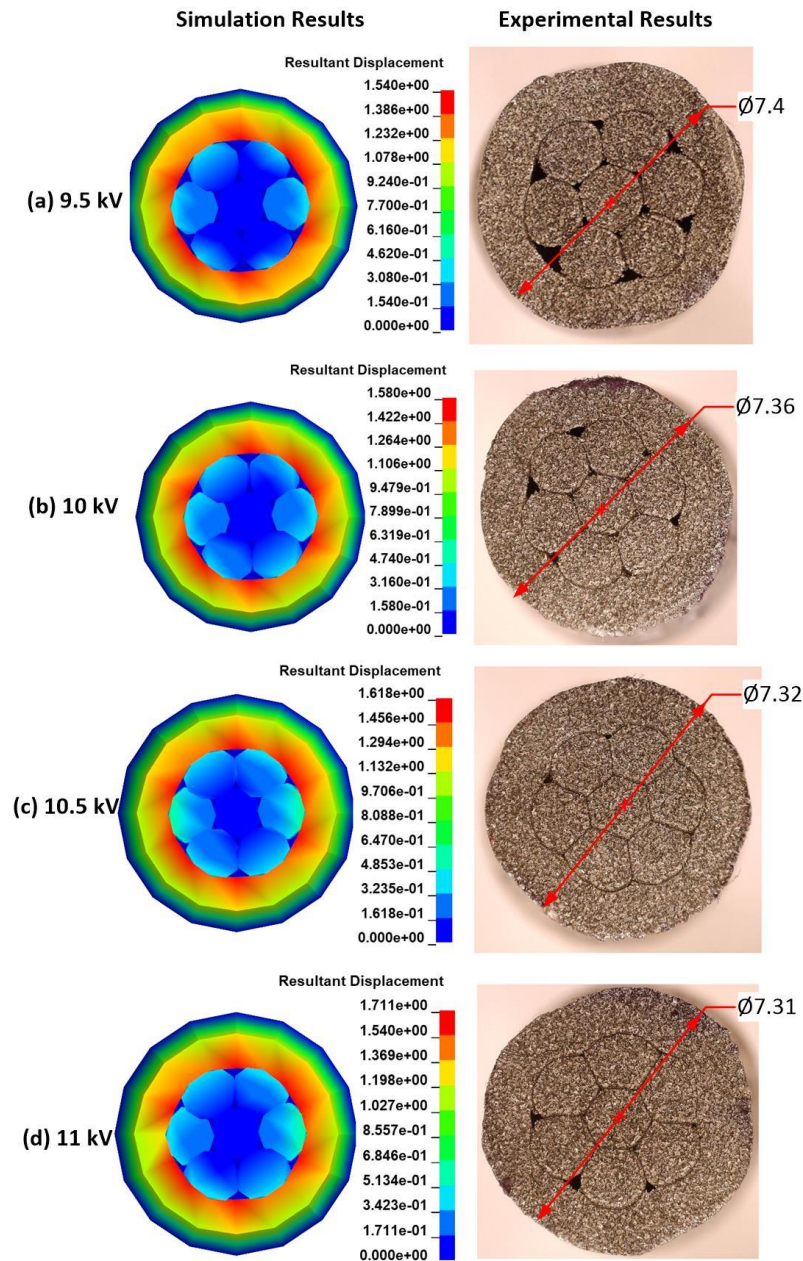
3.4   Radial Deformation

The radial deformation of the terminal increases with the increase in magnetic flux density. As shown in **Figure 10**, the change in radial deformation was found to increase with the increase in discharge voltage for all the three field-shapers because of increase in Lorentz force and the magnetic pressure.
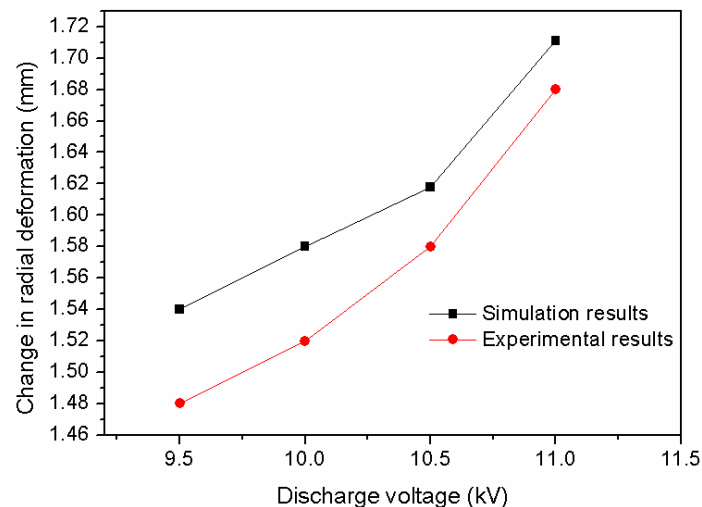
Figure 10: *Variation of change in radial deformation with discharge voltages for three field-shapers*

The Maximum radial deformation of the terminal as per conventional crimping process can be 1.7 mm for these dimensions to avoid dielectric and neutral phase change. Variation of simulation and experimental data for the cross-section analysis is shown **Figure 11**.

Figure 11: Variation in cross-section at different discharge voltages

So, the maximum change in deformation during compression was restricted to 1.70 mm in field-shaper cases. The maximum radial deformation of 1.71 mm was observed in simulation for 11 kV discharge voltage while in an experiment a radial deformation of 1.68 mm was obtained. Minimum voltage at which wire could be constrained inside the terminal was found to be 9.5 kV, wherein experimental radial deformation of 1.48 mm was obtained. So, the voltage range was kept between 9.5 kV to 11 kV for simulation as well as

for the experiments. One essential objective of EM terminal-wire crimping process is to achieve uniform deformation of the terminal over the wire strands. This uniform deformation helps to minimise the voids between the terminal and the wire strands. It can be seen, that with the increase in discharge voltage, radial deformation increase and the gap between the interfaces decreases. Simulation results are in good agreement with the experimental results.

4 Conclusions

In this research article, an alternative to existing conventional terminal-wire crimping process is proposed to overcome the limitations such as non-uniform terminal deformation, indention marks, spring back of the terminal, poor wire strands compaction etc. Electromagnetic crimping process is found to be a most suited process to overcome these issues. Work was carried out on eccentric field-shapers for electromagnetic terminal –wire crimping process. A numerical model was developed in LS-DYNA^{TM} electromagnetic module and results were used for carrying out the experimental work. The current density of 27.45 kA/mm^2 over the effective working zone of field-shaper, induced a magnetic field of 12.64 T over the terminal, Lorentz force of 232 N over the terminal, and radial terminal deformation of 1.7 mm was obtained in simulation results. Radial displacement of the terminal and the cross-sectional cut contact length of the terminal and wire strands obtained in the experimental and the simulations were in good agreement with each other. This design of field-shaper can be used for similar applications. Size of the field shaper is 43 mm and a diameter of 36 mm can easily be manufactured and can be a good alternative option for helical coils which are more prone to dimension change at higher discharge voltages.

References

Bahmani, M A, K Niayesh, and A. Karimi. 2009. "3D Simulation of Magnetic Field Distribution in Electromagnetic Forming Systems with Field-Shaper." Journal of Materials Processing Technology 209: 2295-2301.

Haiping, Yu, Li Chunfeng, and DENG Jianghua. 2009. "Sequential Coupling Simulation for Electromagnetic–Mechanical Tube Compression by Finite Element Analysis." Journal of Materials Processing Technolgy 209: 707-713.

Hustad, T A, and A. L Lindland. 2014. "Aluminium Structures Exposed to Blast Loading." Master's Thesis, Institutt for Konstruksjonsteknikk, Norway.

L Eplattenier, P , G Cook, C Ashcraft, M Burger, J Imbert, and M Worswick. 2009. "Introduction of an Electromagnetism Module in LS-Dyna for Couple Mechanical-Thermal-Electromagnetic Simulations." Steel Research International 80 (5).

Padmanabhan, M. 1997. "Wrinkling and Springback in Electromagnetic Sheet Metal Forming and Electromagnetic Ring Expansion." Master Thesis, The Ohio State University, Ohio.

Psyk, V, D Risch, B L Kinsey, A. E Tekkaya, and M Kleiner. 2011. "Electromagnetic Forming—A Review." Journal of Materials Processing Technology 211 (5): 787-829.

Rajak, A.K., Kore, S.D., 2017. Experimental investigation of aluminium–copper wire crimping with electromagnetic process: Its advantages over conventional process. Journal of Manufacturing Process 26(2017), 57–66.

Suzuki, Hideo, Makoto Murata, and Hideaki Negishi. 1987. "The Effect of a Field Shaper in Electromagnetic Tube Bulging." Journal of Mechanical Working Technology 15: 229-240.

Zhang, H, M Murata, and H Suzuki. 1995. "Effects of Various Working Conditions on Tube Bulging by Electromagnetic Forming." Journal of Materials Processing Technology 48 (1-4): 113-121.

Zhmurkin, D V, N E Corman, C D Copper, and R D Hilty. 2008. "3-Dimensional Numerical Simulation of Open-Barrel Crimping Process." Electrical Contacts, Proceedings of the 54th IEEE Holm Conference on Electrical Contacts. Orlando, FL, USA. 178-184.